HOLOGRAPHIC TWO-WAVELENGTHS INTERFEROMETRY FOR MEASUREMENT OF COMBINED HEAT AND MASS TRANSFER

F. MAYINGER
W. PANKNIN
Institut für Verfahrenstechnik der T.U. Hannover

The two-wavelengths technique was already used a couple of years ago by Ross and El-Wakil (Refs. 1 and 2) for the study of a simulated drop of fuel, but then dropped because of different difficulties involved. However, this technique is so fascinating that we again tried to put the idea into practice by means of using holographic interferometry, instead of Mach-Zehnder interferometry. We thought that both some further theoretical work concerning the evaluation of the interferograms and some experimental improvements would make this measuring technique fit for use.

All interference methods, both the classical ones - as there are Michelson and Mach-Zehnder techniques - and holographic interference techniques first allow only the measurement of refraction index changes in the test section. Only if the reference field is known and if the refraction index was changed only by temperature or concentration or pressure, the interferograms can be evaluated without additional assumptions or measurements. In chemical engineering and combustion research there are however many processes where heat and mass transfer occur simultaneously. Since in all these cases the refraction index is influenced by temperature and concentration changes simultaneously, additional information is needed for the evaluation of the interferograms. The combination of interferometry with conventional measuring techniques using probes or thermocouples has severe drawbacks. The devices can disturb the process, are often not fast enough for the measurement of rapid events, or they are too big to allow examinations in thin boundary layers

It is therefore desirable to try to obtain the additional information also by using optical techniques.

Since the refraction index is a function of the wavelength, the idea of two-wavelengths technique is, to take two interferograms simultaneously in

order to determine both temperature and concentrations of two-component systems from the difference of the interferograms. This principle was already successfully used in plasma physics to determine the electron and ion density of a plasma (Ref. 3).

The substances which one usually encounters in combined heat and mass transfer, however, have a much smaller dependance of the refraction index on the wavelength of light as one finds when examining a plasma. Therefore the optical set up, the measurement of the interference orders and the evaluation of the interferograms requires much more accuracy than usually needed in one-wavelength techniques. Holography provides much help to overcome the experimental difficulties and thus enables many more problems to be examined by using this technique. First the evaluation equations and the necessary corrections of the interferograms shall be discussed. Then the experimental set up will be explained and some applications will be given.

From the interferograms, which were made for example by using the double exposure technique, one first gets the changes of the optical path along the light beam (Ref. 1). S is the interference order in multiples of a wavelength λ. If we assume a straight light path and a constant field during the exposure of the comparison field, the equation can be integrated if a two dimensional field (constant in light beam direction) is provided. We then obtain Eq. 2 which is the equation of ideal interferometry. If gases are to be examined the Gladstone Dale equation gives the relation between refraction index and density. Using in addition the ideal gas law we obtain Eq. 3, where N is the molar refractivity. This molar refractivity is the sum of the refractivities of the pure components a and b in the mixture. Eq. 4 gives the relation between fringe shift S temperature T and concentration C. Since N is a function of wavelength, two interferograms taken at different wavelengths λ_j and λ_k allow to eliminate one of the unknowns T or C. From Eq. 5 temperature T can be obtained by evaluating both interferograms.

In Fig. 3 the principle of evaluation is demonstrated schematically. Two interferograms with fringe shifts $s_j\lambda_j$ and $s_k\lambda_k$ are recorded.

The difference of the product $S\frac{\lambda}{N}$ is a value for $\frac{C}{T}$ The concentration C can be found also by using the temperature and only one interferogram.

The picture already indicates that the measuring effect is very small. It mainly depends on the optical properties of the system. In order to obtain good measuring accuracies the deviations from ideal interferometry must therefore be taken into consideration. Three effects will be discussed.

First we consider the case that the boundary layer extends over the actual test length. Therefore the light beam receives an additional fringe shift ΔS. This correction term can be calculated by representing the measured fringe shift curve by a polynominal of e.g. 5th order and integrating Eq. 1 in Fig. 4. In two wavelength interferometry the differences of the two interferograms give the measuring value. The ratio of $\Delta S_j\lambda_j$ and $\Delta S_k\lambda_k$ depends on whether the fringe shift is mainly due to concentration or temperature changes.

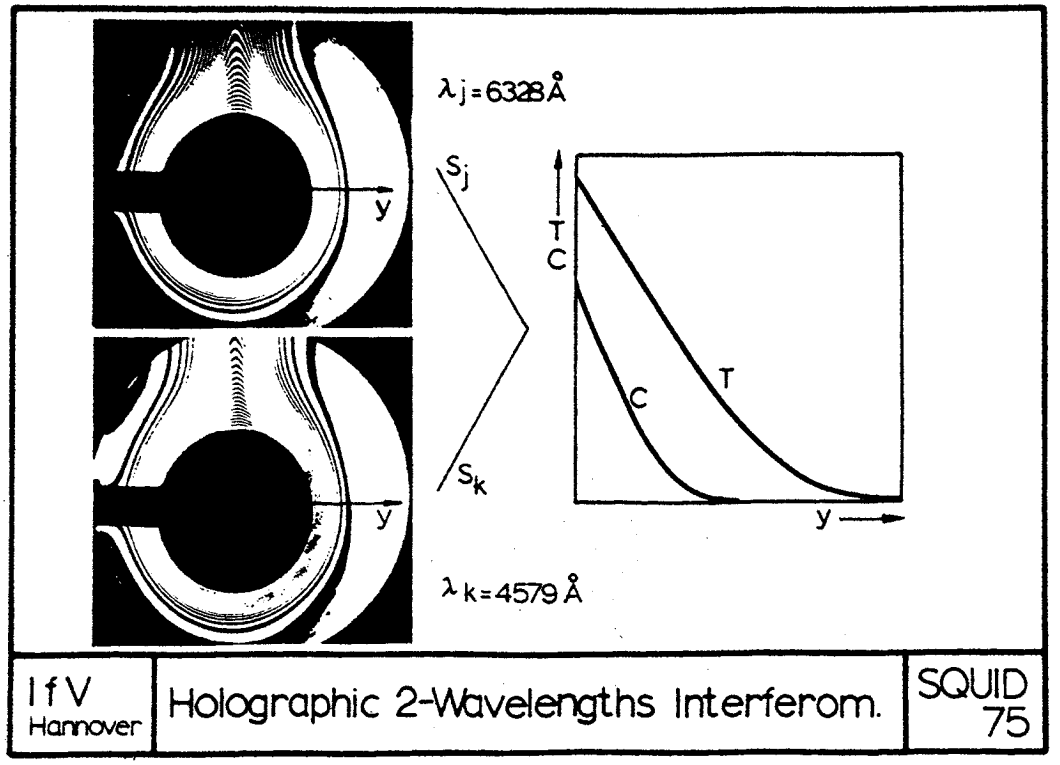
λj=6328Å
Sj
Sk
λk=4579Å
y
y
T
C
C
T
y
IfV Hannover
Holographic 2-Wavelengths Interferom.
SQUID 75

Fig. 1

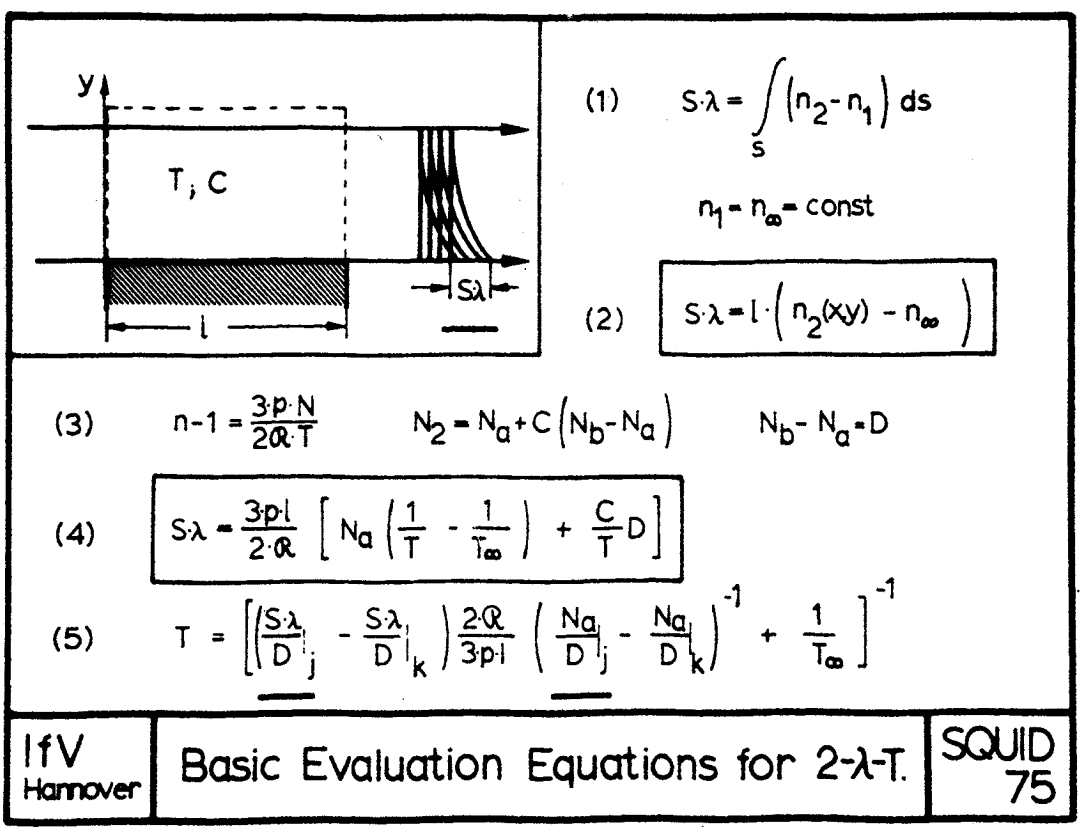
y
T; C
l
Sλ
(1) $S\cdot\lambda = \int_s (n_2 - n_1)\, ds$
$n_1 = n_\infty = \text{const}$
(2) $S\cdot\lambda = l\cdot(n_2(x,y) - n_\infty)$
(3) $n-1 = \frac{3\cdot p\cdot N}{2\cdot R\cdot T}$ $N_2 = N_a + C(N_b - N_a)$ $N_b - N_a = D$
(4) $S\cdot\lambda = \frac{3\cdot p\cdot l}{2\cdot R}\left[N_a\left(\frac{1}{T} - \frac{1}{T_\infty}\right) + \frac{C}{T}D\right]$
(5) $T = \left[\left(\frac{S\cdot\lambda}{D}\Big|_j - \frac{S\cdot\lambda}{D}\Big|_k\right)\frac{2\cdot R}{3\cdot p\cdot l}\left(\frac{N_a}{D}\Big|_j - \frac{N_a}{D}\Big|_k\right)^{-1} + \frac{1}{T_\infty}\right]^{-1}$
IfV Hannover
Basic Evaluation Equations for 2-λ-T.
SQUID 75

Fig. 2

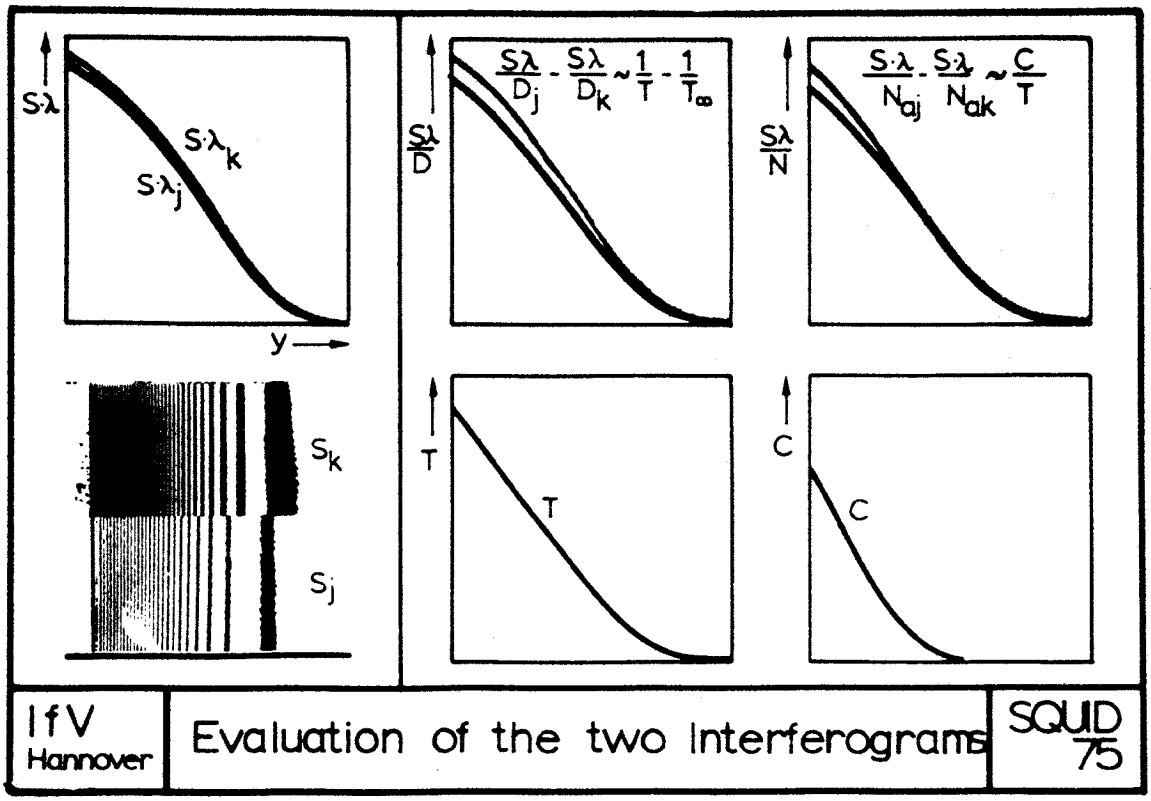

Fig. 3

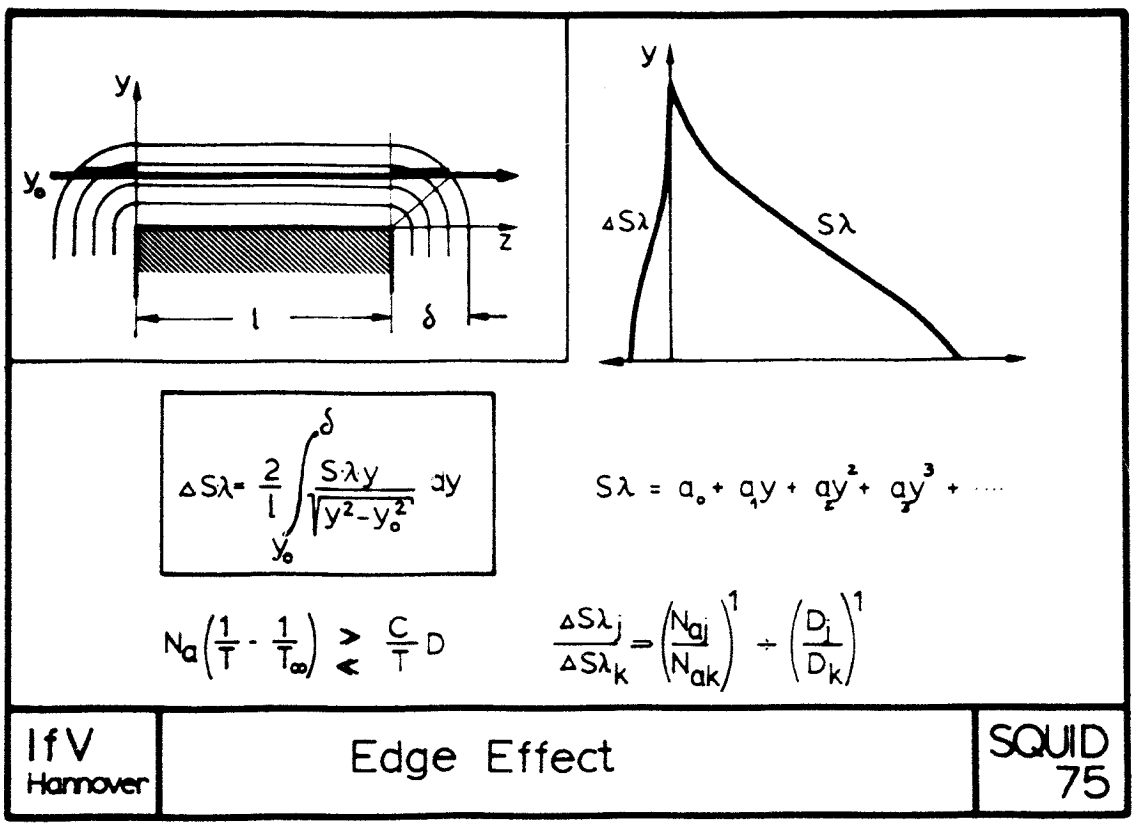

$$\Delta S\lambda = \frac{2}{l}\int_{y_0}^{\delta} \frac{S\lambda\, y}{\sqrt{y^2 - y_0^2}}\, dy$$

$$S\lambda = a_0 + a_1 y + a_2 y^2 + a_3 y^3 + \cdots$$

$$N_a\left(\frac{1}{T} - \frac{1}{T_\infty}\right) \gtrless \frac{C}{T} D$$

$$\frac{\Delta S\lambda_j}{\Delta S\lambda_k} = \left(\frac{N_{aj}}{N_{ak}}\right)^1 \div \left(\frac{D_j}{D_k}\right)^1$$

Fig. 4

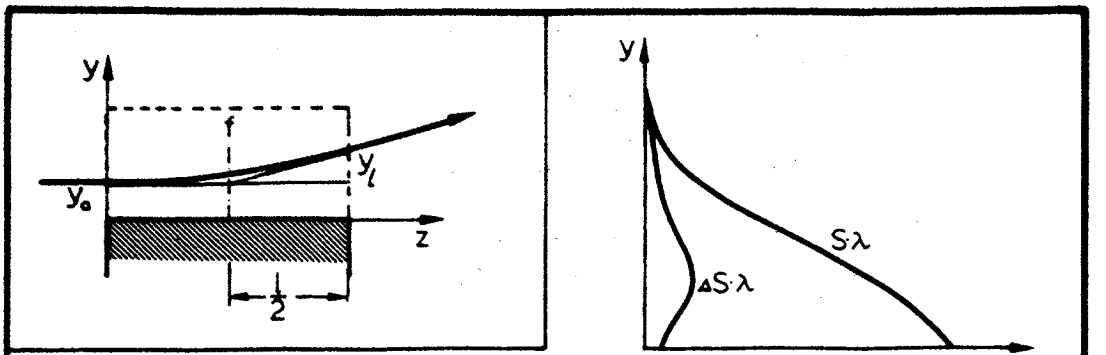

(1) $n = n_o + n'(y - y_o) \qquad y_o \le y \le y_l$

(2) $\boxed{\Delta S\cdot\lambda = \frac{S'^2\cdot\lambda^2}{12\, n_o}\, l} \qquad l_f = \frac{l}{2}$

$N_a\left(\frac{1}{T} - \frac{1}{T_\infty}\right) \gtrless \frac{C}{T} D \qquad \frac{\Delta S\lambda_j}{\Delta S\lambda_k} = \left(\frac{N_{aj}}{N_{ak}}\right)^2 \div \left(\frac{D_j}{D_k}\right)^2$

IfV Hannover	Light Deflection Effect	SQUID 75

Fig. 5

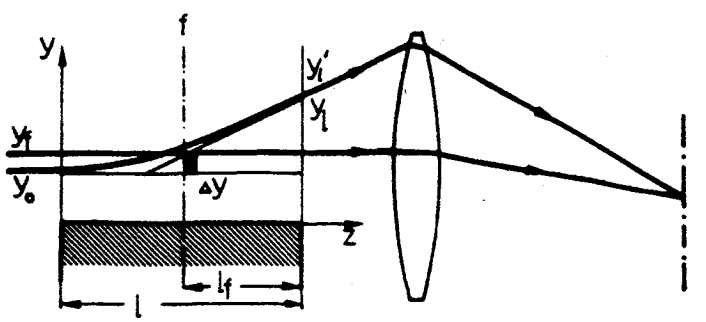

(1) $\boxed{\Delta y = y_f - y_o}$

$\Delta y = y_l - y_o - \left(\frac{dy}{dz}\right)_l \cdot l_f$

(2) $n = n_o + n'(y - y_o) + n''\frac{1}{2}(y - y_o)^2 \longrightarrow \frac{1+y'^2}{1+y_o'^2} = \left(\frac{n}{n_o}\right)^2 \longrightarrow y_l ; y_l'$

(3) $\boxed{\Delta y = \frac{n'}{n_o} l\left(\frac{l}{2} - l_f\right) + \frac{n' n''}{n_o n_o} \frac{l^3}{6}\left(\frac{l}{4} - l_f\right)} \qquad \Delta S\cdot\lambda = \Delta y \cdot S'\lambda$

(4) $N\left(\frac{1}{T} - \frac{1}{T_\infty}\right) \gtrless \frac{C}{T} D \qquad \frac{\Delta S\lambda_j}{\Delta S\lambda_k} = \left(\frac{N_{aj}}{N_{ak}}\right)^3 \div \left(\frac{D_j}{D_k}\right)^3$

IfV Hannover	Displacement Error Δy	SQUID 75

Fig. 6

This can be determined using an iterative way of solution, by neglecting first all the correction terms.

An additional fringe shift is due to the fact that the light beam is deflected towards the denser optical fluid. If we assume that within this region of deflection the refraction index can be represented by Eq. 1 the additional fringe shift is calculated by using Eq. 2. In this case we have, focussed onto the middle of the test section. The ratio of the correction terms is now proportional to

$$\left(\frac{Na_j}{Na_k}\right)^2 \text{ or } \left(\frac{D_j}{D_k}\right)^2$$

Connected with the light deflection is a displacement λ_y of the interference lines. The beam which enters the test section at y_o is photographed at the position y_f. This is dependent on the focusing length l_f. If the refraction index is described by Eq. 2, the general equation for the light beam can be solved (Ref. 4, 5) and we get the exit values. The correction term 3 gives us the displacement error as a function of focusing length. Focusing onto the middle of the section gives the minimum displacement, which is a function of n' and n". The additional fringe shift is now proportional to

$$\left(\frac{Na_j}{Na_k}\right)^3 \text{ or } \left(\frac{D_j}{D_k}\right)^3$$

A more refined analysis is given in (Ref. 6) where the third order terms are also applied to the calculation of fringe shift $\Delta S\lambda$ in Fig. 5. The final result then is that the overall correction term is a minimum for $l_F = 1/3$, with $\Delta S\lambda = n'^2\, n''\, \ell^5\, 1/30$. The distribution of this correction term is shown schematically in Fig. 7.

From the smooth temperature and concentration profiles a smooth fringe shift curve S results. The correction term is however proportional to the product of s' and s", and results in relatively strong local deviations of the measured values, which can lead to considerable errors in the final evaluation procedure. This was confirmed experimentally.

In Fig. 8 the measured fringe width b is plotted for the wall next boundary layer. The deviations from the theoretical straight curve lead to mistakes when the gradient near the wall is to be determined. Since both interferograms are affected, the resultant mistake can be kept small by careful interpolation between the fringes.

The experimental holographic set up is shown schematically in Fig. 9. It differs from conventional arrangements only by using two lasers simultaneously. The beams of a He-Ne-Laser and an Argon Laser are superposed in a beam splitter S. Then the beams are divided into reference wave RW and object wave OW, both with two wavelengths. The object beam passes through the test section TS and both waves interfere on the hologram H. When a double exposure is made, having a constant field first and introducing the heat and mass transfer before the second exposure, the hologram can be reconstructed afterwards. The two

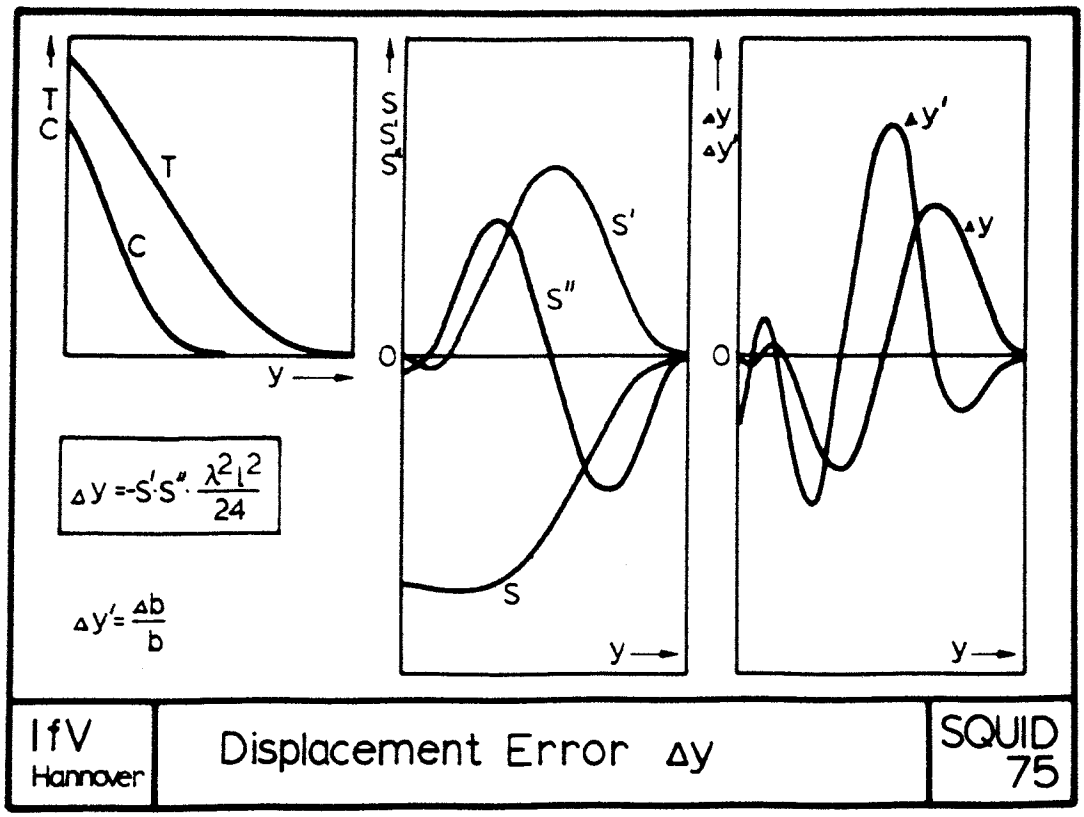
T
C
T
C
y
S
S'
S''
S
0
y
Δy
Δy'
Δy'
Δy
0
y
Δy = -S'S'' · λ²l²/24
Δy' = Δb/b
IfV Hannover
Displacement Error Δy
SQUID 75

Fig. 7

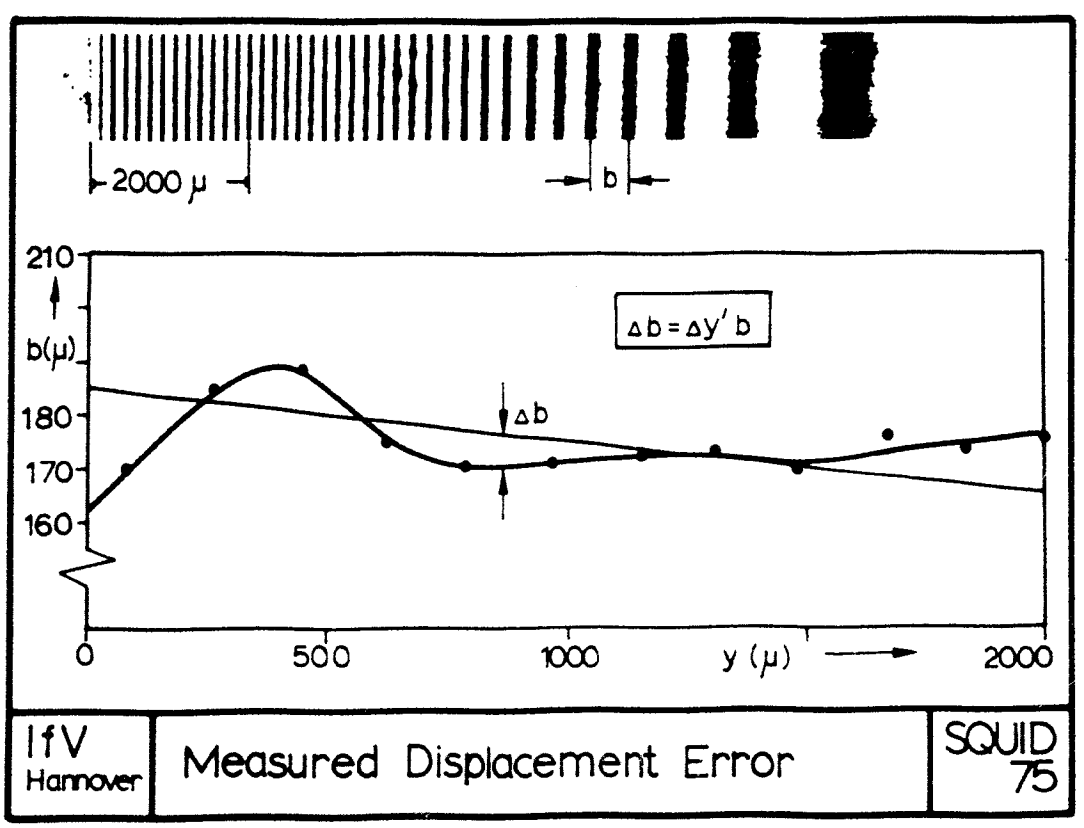
2000 μ
b
210
b(μ)
180
170
160
Δb = Δy' b
Δb
0
500
1000
y (μ)
2000
IfV Hannover
Measured Displacement Error
SQUID 75

Fig. 8

resultant negatives. This is usually done by means of a microscope or photometer.

This procedure is easy, has however an important drawback. It is nearly impossible to get an exact reference line for the two interferograms. This problem was already encountered by Ross (Ref. 1). It can lead to a displacement of the two fringe shift curves to one another, resulting in enormous mistakes.

Therefore a modified holographic set up was developed and tested.

The two interferograms are projected in this set up onto the hologram by placing the camera lens between test section and hologram. The step of taking sharp pictures by using the lens was thus combined with the recording of the hologram. The hologram itself can now be used for measuring the fringe positions. This is done by illuminating it under a photometer alternately with the two reference beams. This guarantees an exact correspondence of the fringe shifts and improves considerably the obtainable accuracy.

It may be mentioned that both techniques result in interferograms which are as crisp and sharp as in classical Mach Zehnder interferometry. All one has to do is to carefully allign the optical set up and to eliminate interference patterns due to dust particles by using a pin hole in the focus of the beam expanding lenses. Recent results show that interference lines with a fringe width of less than 30μ can be recorded and evaluated (Ref. 7).

In Fig. 11 the resultant interferograms of a heat and mass transfer boundary layer are shown. The model consisted of a heated horizontal cylinder covered by a thin layer of subliming naphtalene. Many of such interferograms as well as interferograms obtained for heat and mass transfer on a vertical plate were evaluated. One typical example is given in Fig. 12 where the resulting temperature and concentration profiles correspond exactly to the wall values, which were determined by extra measurements. Experimentally determined Sherwood and Nusselt Numbers are given in Fig. 13. The values are in good agreement with theoretical investigations as e.g. by Wilcox (Ref. 8). The deviations are mainly due to the fact that for obtaining the Nu and Sh-numbers the gradient of the temperature and concentration profiles had to be determined near the wall, which can lead to some errors. The evaluation technique was not the iterative way, proposed by Ross (Ref. 1) but the simultaneous solution of the two interferograms.

When we got the invitation to this workshop we had only few time to apply the two wavelength technique to the study of combustion phenomena. However the results obtained within this short period may indicate how well this technique works. The technique was used for the investigation of temperature and fuel vapour concentration in a simulated drop of fuel, as earlier done by Ross.

Fig. 14 shows the dual interferograms of a burning n-Hexan cylinder. The model consisted of a porous bronze cylinder of 9 mm ø and 50 mm length, through which the fuel evaporated. Since the light beam near the surface is deflected

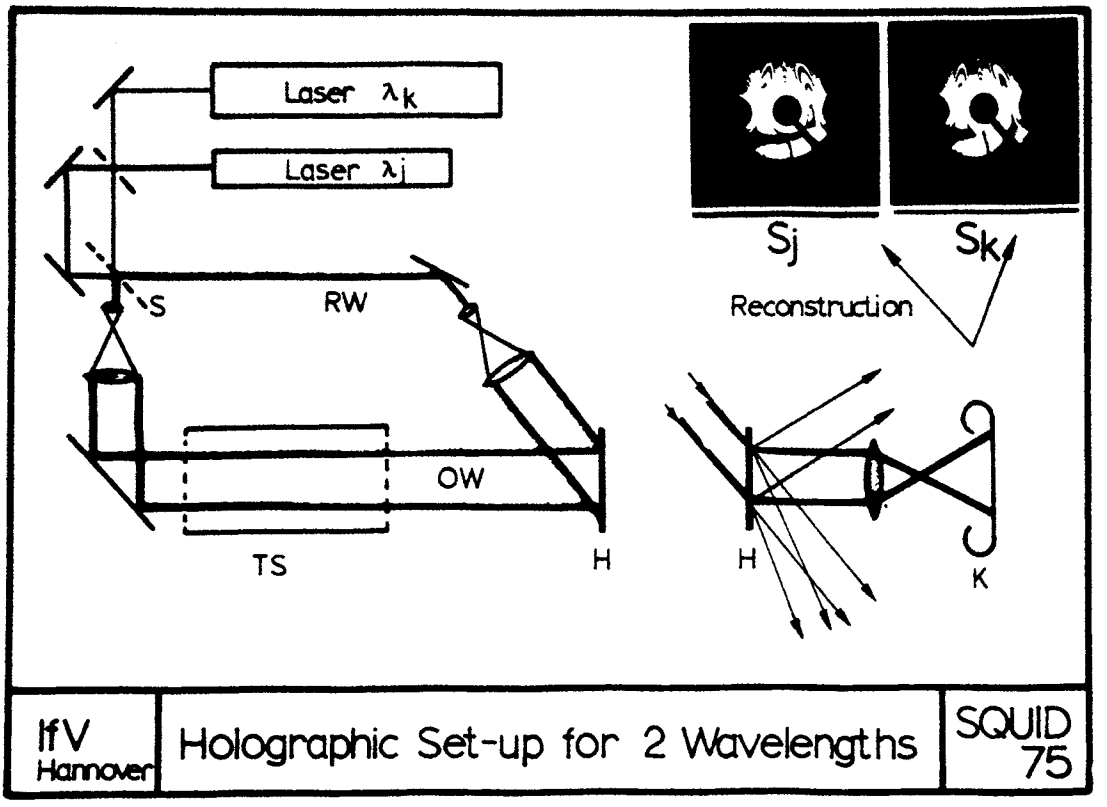
Laser λ_k
Laser λ_j
S
RW
OW
TS
H
Sj
Sk
Reconstruction
H
K
IfV Hannover
Holographic Set-up for 2 Wavelengths
SQUID 75

Fig. 9

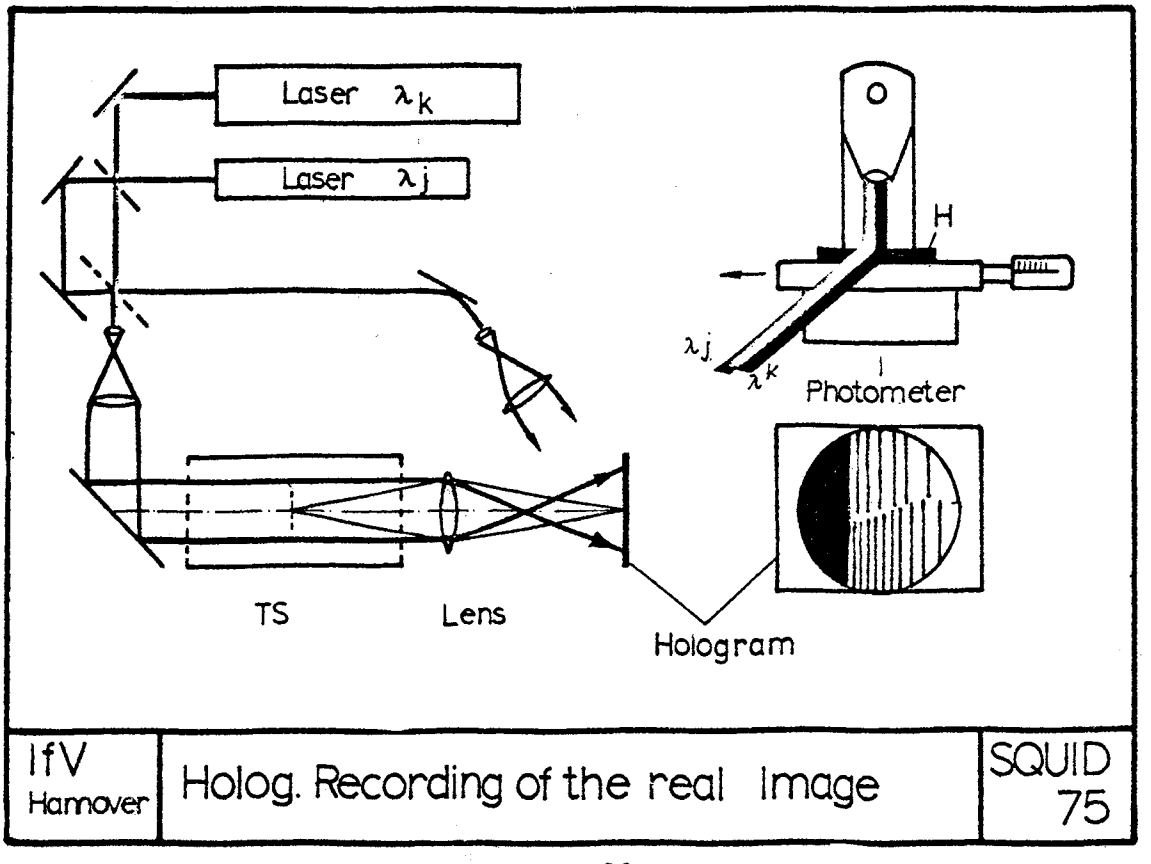
Laser λ_k
Laser λ_j
O
H
λ_j
λ_k
Photometer
TS
Lens
Hologram
IfV Hannover
Holog. Recording of the real Image
SQUID 75

Fig. 10

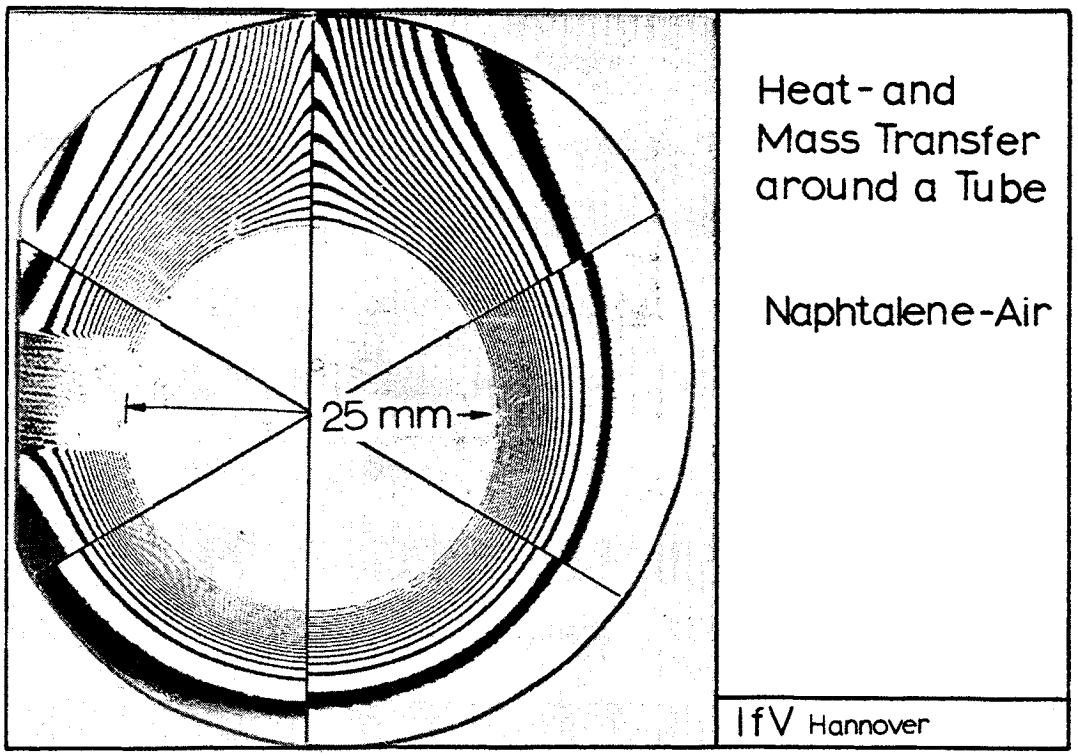
25 mm
Heat-and
Mass Transfer
around a Tube
Naphtalene-Air
IfV Hannover

Fig. 11

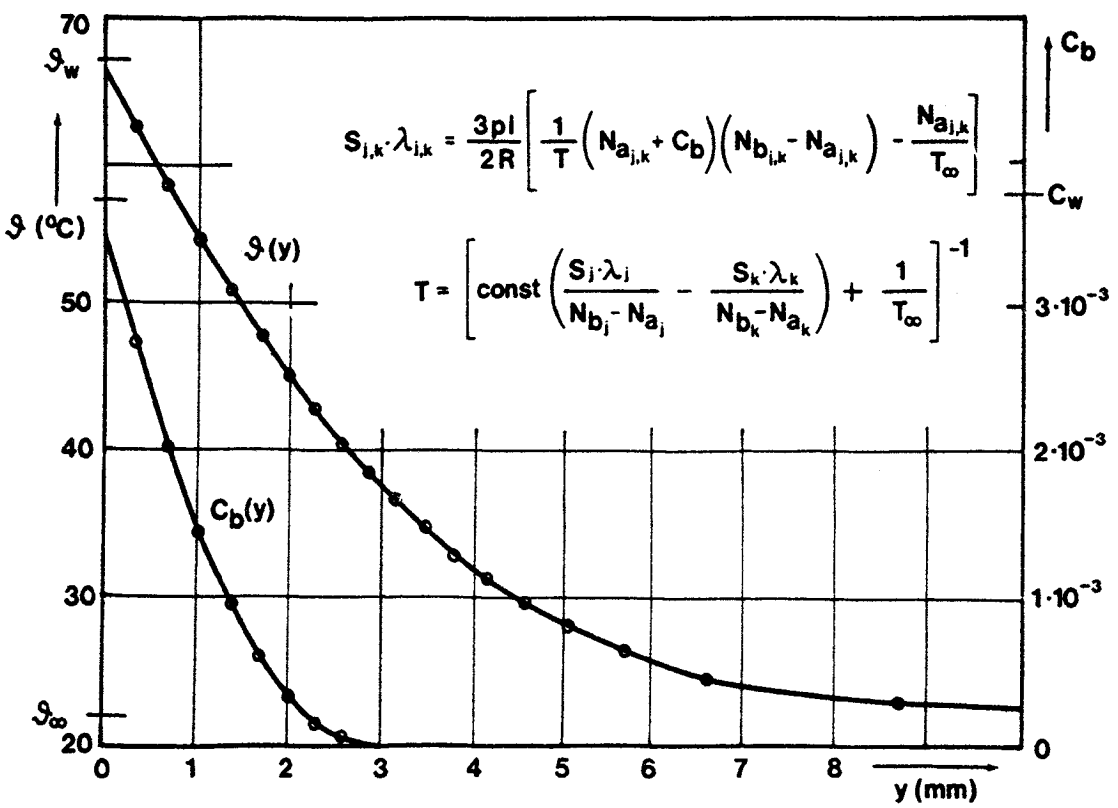
70
ϑ_w
ϑ (°C)
50
40
30
ϑ_∞
20
0
1
2
3
4
5
6
7
8
y (mm)
ϑ(y)
C_b(y)
C_b
C_w
$3\cdot10^{-3}$
$2\cdot10^{-3}$
$1\cdot10^{-3}$
0
$S_{j,k}\cdot\lambda_{j,k} = \frac{3pl}{2R}\left[\frac{1}{T}\left(Na_{j,k}+C_b\right)\left(Nb_{j,k}-Na_{j,k}\right)-\frac{Na_{j,k}}{T_\infty}\right]$
$T=\left[\text{const}\left(\frac{S_j\cdot\lambda_j}{Nb_j-Na_j}-\frac{S_k\cdot\lambda_k}{Nb_k-Na_k}\right)+\frac{1}{T_\infty}\right]^{-1}$

Fig. 12

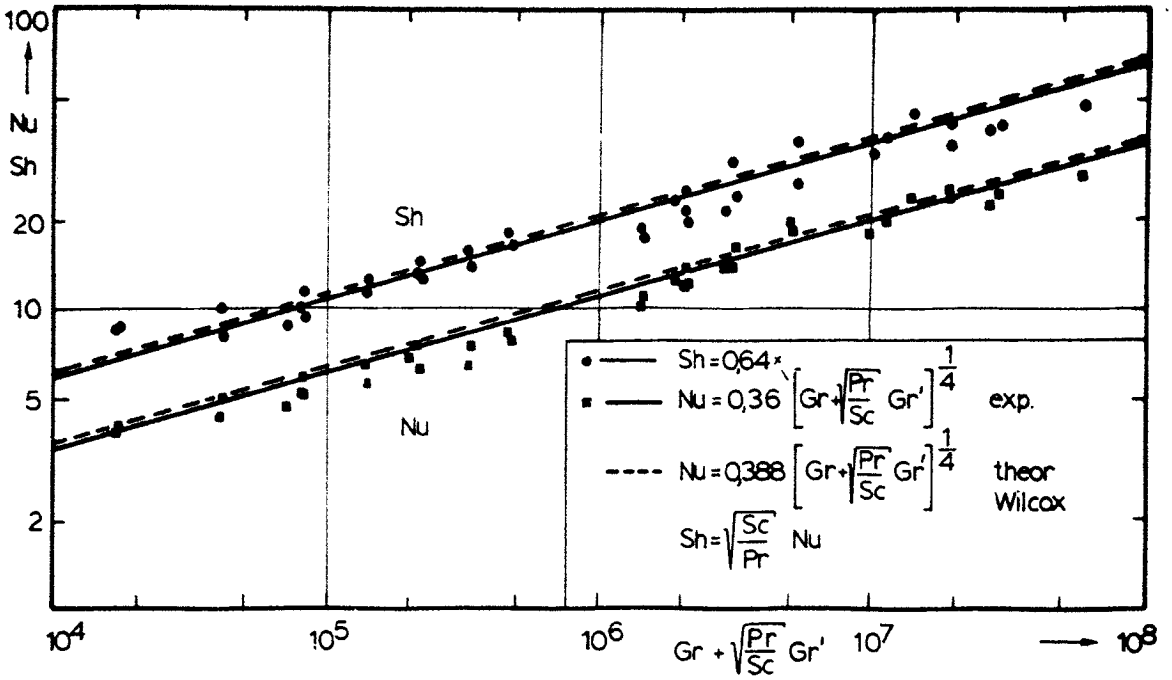

IfV Hannover	Heat-and Mass Transfer on Vertical Wall	SQUID 75

Fig. 13

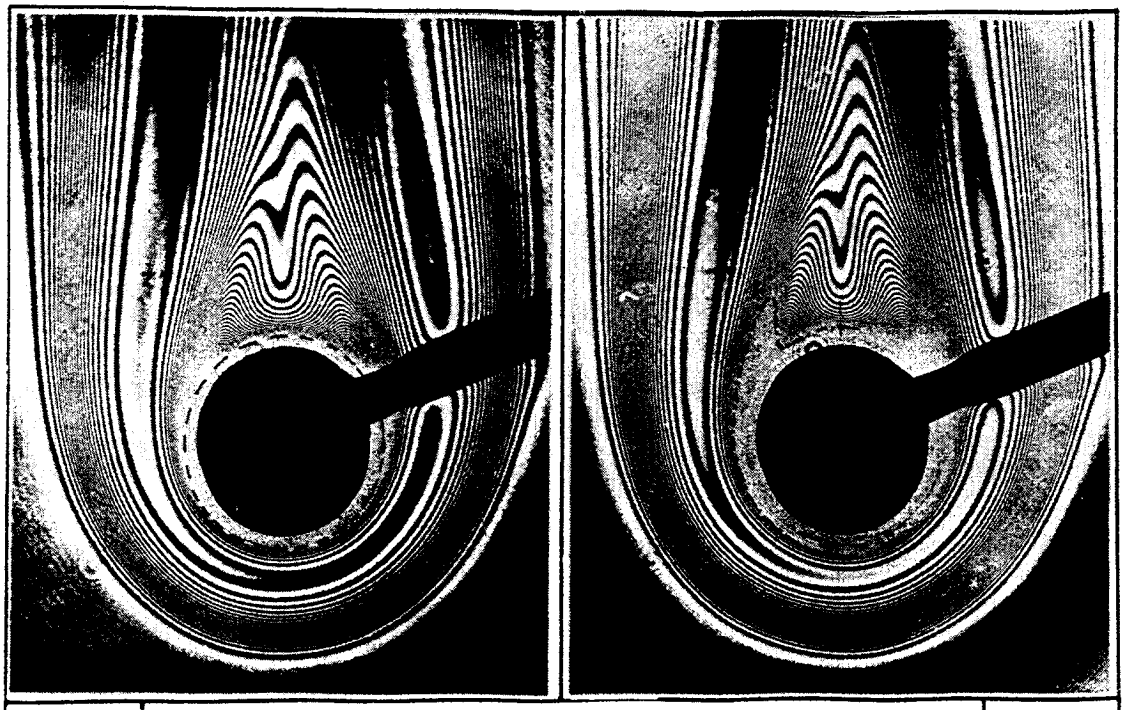

IfV Hannover	Interferograms of Burning n-Hexan Cylinder	SQUID 75

Fig. 14

into the surface (dashed circle) only outside of this region the boundary layer could be studied.

The fuel n-Hexan is not well suited for the two wavelength technique because of the very low dependance of the refraction index on the wavelength. Nevertheless the evaluation of the dual interferograms showed that the concentration of fuel vapour reached nearly zero at the distance 1.5 mm from the wall at the position 0^{o} and about 3 mm from the wall at position 135^{o}. Therefore within this reaction zone the temperature was obtained by using one interferogram only. The fringe shift could be determined until near the wall where the fringe density is about 50 lines per mm which is an improvement compared to the results of Ross.

Additional thermocouple measurements confirmed the interferometric results. The region of fuel vapour can be estimated roughly by determining the fringe width curve. The beginning of the reaction zone is connected with the beginning of heat production and thus with a sudden change of the temperature and concentration gradient. This results in a sudden change of fringe density too, which can be seen in picture 14B indicated by the dotted curve.

First evaluations indicate that the fuel vapour concentration along this curve reaches values of about 0,2. The results obtained so far are in good agreement with measurements of Ross and the results reported in this workshop by El-Wakil who used gas chromatography as measuring technique.

The final picture may indicate some more applications of holography. A double exposure hologram is compared to a single exposure hologram. This was obtained by using a relatively long exposure time (1/50 sec). The interference lines which are seen in the right picture are lines due to the changing of the wavefront during the exposure time. The fringe density is proportional to wavefront gradient and the velocity of change. Further theoretical work in this very new field might reveal this to be a powerful technique for the study of flame front velocities and instationary reaction zones.

The use of two wavelength holography turned out to be a fine measuring technique for the study of simultaneous heat and mass transfer. The refined evaluation techniques and the better experimental arrangement allow the investigation even of mixtures whose optical properties do not vary much with the wavelength. This was confirmed by investigating air naphtalene and air-n-Hexan mixtures.

The development of tunable gas-lasers which allow a farther spread of wavelength, and the use of pulsed ruby lasers with frequency doubling promises an even larger field of applications of holographic two-wavelength interferometry. In this report only holographic two-wavelength technique was spoken about. As a participant of the workshop I think that all the other applications of holographic interferometry as well as holographic particle determination techniques were not discussed sufficiently enough.

We may therefore refer to some more of our own applications and experiences which were published in (Ref. 9, 10, 11).

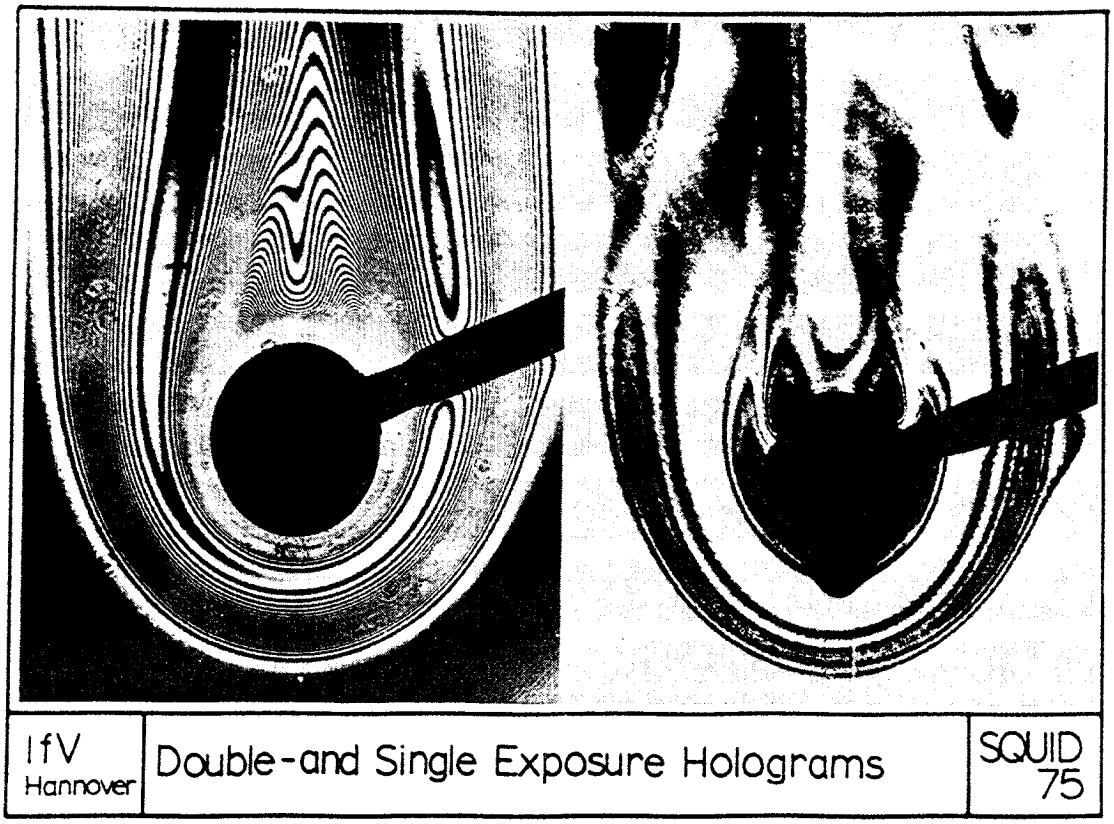
IfV
Hannover
Double-and Single Exposure Holograms
SQUID
75

Fig. 15

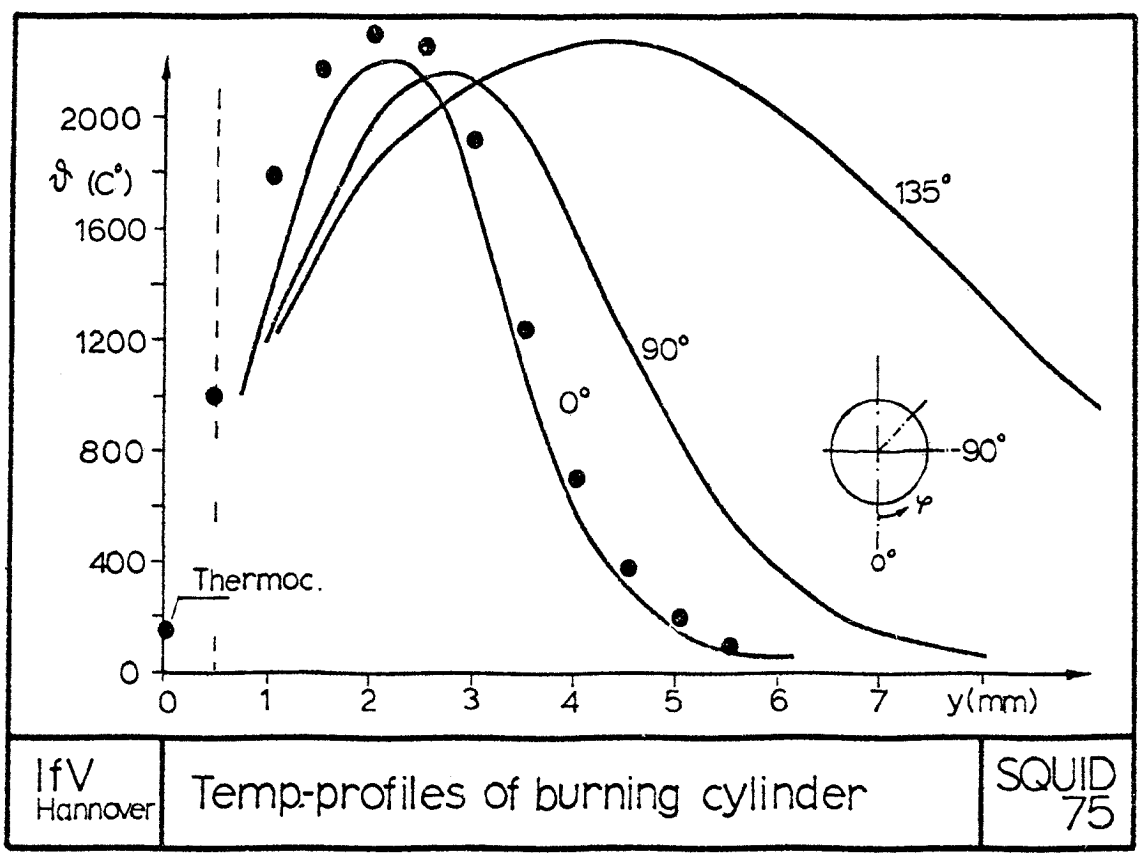
2000
ϑ (C°)
1600
1200
800
400
0
Thermoc.
0
1
2
3
4
5
6
7
y(mm)
135°
90°
0°
-90°
φ
0°
IfV
Hannover
Temp-profiles of burning cylinder
SQUID
75

Fig. 16

References

1. P. A. Ross, Application of a two-wavelength interferometer to the study of a simulated drop of fuel. PhD thesis, University of Wisconsin (1960)

2. M. M. El-Wakil and P. A. Ross, A Two Wavelength Interferometric Technique for the Study of Vaporization and Combustion of Fuels, Liquid Rockets and Propellanta: Progress in Astronautics and Rocketry, Vol. II, Academic Press, New York (1960)

3. D. Meiners and C. O. Weiss, Interferometrische Messung der thermischen ZustandsgroBen von EdelgasstoBwellenplasmen. Z. Naturforschun, 28 a, 8, (1973)

4. U. Grigull, Einige optische Eigenschaften thermischer Grenzschichten, Intern J. Heat Mass Transfer 6, (1963)

5. W. Hauf and U. Grigull, Optical Methods in Heat Transfer Advances in Heat Transfer 6, (1970)

6. W. Panknin, Dissertation, Hannover

7. F. Mayinger and W. Panknin, Holography in Heat and Mass Transfer. Proceedings of the 5th Int. Heat Transfer Conf. Tokio (1974)

8. W. R. Wilcox, chem. Eng. Sci. 13,3,113 (1961)

9. W. Panknin, Einige Techniken und Anwendungen der holgraphischen Durchlichtinterferometrie CZ-Chemie Technik, 3 (1974)

10. W. Panknin, M. Jahn u. H. H. Reineke, Forced Convection Heat Transfer in the Transition form Laminar to Turbulent Flow in Closely Spaced Circular Tube Bundles, 5th Int. Heat Transfer Conf., Tokio (1974)

11. F. Mayinger, D. Nordmann u. W. Panknin, Chem. Ing. Tech. 46 (1974)